World Academy of Science, Engineering and Technology
International Journal of Materials and Metallurgical Engineering
Vol:12, No:11, 2018

A Numerical Method to Evaluate the Elastoplastic Material Properties of Fiber Reinforced Composite

M. Palizvan, M. H. Sadr, M. T. Abadi

Abstract**—**The representative volume element (RVE) plays a central role in the mechanics of random heterogeneous materials with a view to predicting their effective properties. In this paper, a computational homogenization methodology, developed to determine effective linear elastic properties of composite materials, is extended to predict the effective nonlinear elastoplastic response of long fiber reinforced composite. Finite element simulations of volumes of different sizes and fiber volume fractures are performed for calculation of the overall response RVE. The dependencies of the overall stress-strain curves on the number of fibers inside the RVE are studied in the 2D cases. Volume averaged stress-strain responses are generated from RVEs and compared with the finite element calculations available in the literature at moderate and high fiber volume fractions. For these materials, the existence of an RVE is demonstrated for the sizes of RVE corresponding to 10–100 times the diameter of the fibers. In addition, the response of small size RVE is found anisotropic, whereas the average of all large ones leads to recover the isotropic material properties.

Keywords**—**Homogenization, periodic boundary condition, elastoplastic properties, RVE.

I. Introduction

THE prediction of the effective elastoplastic response of fibrous composite materials consisting of linear elastic fibers and elastoplastic matrix, such as epoxy matrix composites reinforced with glass fibers, is an important and active research topic (see, e.g., [1]-[3]). Progress in computational techniques of the last decade has provided powerful tools for the solution of this problem. Commercial computational packages like ANSYS and ABAQUS based on the finite element method (FEM) allow one to solve the homogenization problem on the basis of calculation of the detailed stress and strain fields in a RVE of a composite that contains tens of fibers of various shapes and properties. The result of prediction is often presented in the form of stress-strain relation under some simple loading, say, simple tension or pure shear.

Existing methods for predicting the elastoplastic response of composite materials include the secant homogenization method [4], incremental homogenization method based on the Mori–Tanaka model [5], the direct approach using RVEs [2], and periodic unit cell method [6]. The secant method is limited to monotonic and proportional loading. The incremental homogenization method has no such limitation and can be applied to load reversal or cyclic load. However, in its original form, the incremental approach over-predicts elastoplastic stress-strain response and the remedy is to use only the isotropic part of the anisotropic elastoplastic tangent stiffness tensor [5]. However, the use of only the isotropic part of the tangent stiffness tensor, while resulting in much-improved prediction, lacks either theoretical or physical basis. In addition, fitting parameters may be needed in formulating the isotropic part of the tangent stiffness tensor [7]. It is well known that for a particulate composite with its matrix material characterized by the von Mises yield condition (the theory of J2 plasticity), reinforced with homogeneous, isotropic and linearly elastic particles, the composite as a whole may yield under hydrostatic stress even though the matrix does not [8]-[10].

The direct approach using RVEs gives a rigorous prediction of the effective composite elastoplastic response, but is computationally expensive, particularly given the nonlinear nature of plastic deformation. The unit cell method applies to composites with periodic microstructures. It cannot be rigorously applied to real composites which in general are not periodic. Because of its simplicity, the unit cell method is nonetheless often used to approximate the elastoplastic behavior of real composites [11], [12]. In addition to the aforementioned methods, Sun and Ju [13] applied the ensemble averaging approach to the prediction of the effective elastoplastic response of particulate composites.

The primary methods for studying the effective material properties of the RVE include approaches based on analytical homogenization schemes, mainly restricted to linear cases. These techniques (e.g., [14]-[16]) have been used to consider different shapes of inclusions and have been useful in some situations to determine the effective material properties of the RVE with respect to the inclusions' characteristics. On the other hand, some approaches based on numerical methods, such as the FEM (e.g., [17]-[20]), use computations on a unit cell and allow determining the size of the RVE via statistical analyses relying on numerical computations. These techniques have been mainly applied in the linear case, and a few recent studies involve nonlinear heterogeneous materials. For linear composites, determining the size of the RVE can be performed by analyzing the statistical convergence of effective material parameters with respect to the size of the unit cell. Kanit et al. [21] studied the linear thermal and elastic properties of random 3D polycrystalline microstructures. Ranganathan and Ostoja-Starzewski [22] investigated random polycrystal microstructures made up of cubic single crystals. Other examples in elasticity can be found in [23]-[27]. In [28], new

M. Palizvan is with the Aerospace Research Institute, Tehran, Iran (corresponding author, e-mail: palizvan@sun.ari.ac.ir).

M.H. Sadr is with the Aerospace Engineering Department, Amirkabir University of Technology, Tehran, Iran (e-mail: Sadr@aut.ac.ir).

M.H. Sadr and M. T. Abadi are with the Department of Aerospace Engineering (Structural design), Aerospace Research Institute, Tehran, Iran (e-mail: Homayoune.sadr@ari.ac.ir, Abadi@ari.ac.ir).

criteria to determine the size of RVE with random elastic matrix have been proposed as well as estimates for RVE sizes. In [29], a stochastic homogenization theory has been introduced for random anisotropic elastic composites that cannot be described in terms of their constituents and for which the standard methods cannot be applied, like cortical bones or biological membranes. In [30], a method using the concept of periodization of random media was used to estimate the effective properties of random composites using small volumes.

For nonlinear composites, most of the proposed methodologies are based on analyzing the convergence of the effective response (e.g., the effective stress), computed numerically at one point of the loading curve with respect to the size [31]-[33]. More recent studies analyze the convergence of identified parameters related to an empirical macroscopic model with respect to the unit cell size [34], [35].

Although reliable micromechanics models for linear elastic composites have been available for a long time, developing models approaches for nonlinear composites remains highly challenging. The aim of the present work is to develop a numerical algorithm which is able to simulate, with reasonable accuracy, computer time, and memory the elastoplastic behavior of matrix composite materials. The numerical estimates of the stress-strain response and their scatter obtained on volumes of fixed size but containing different realizations of a given volume of the microstructure are investigated.

The present paper is organized as follows. In Section II, a plasticity model is presented to show how we simulate the mechanical behavior of the matrix, based on available experimental evidence, and also, periodic boundary conditions and numerical homogenization methods are illustrated. The analysis models, computational implementation, and results are presented and discussed in Section III. Some concluding remarks are given in Section IV.

II. Plasticity Theory

The current section provides an overview of the theoretical aspects of plasticity. The books [36]-[39] provide a more detailed and broader perspective on the general theory of plasticity as well as its phenomenological aspects. In this thesis, only small deformations will be considered. This assumption is justified by the presence of cracking for small deformations. Considering only small-strains will also allow simplifying the model's definition and implementation.

Fig. 1 shows the mathematical idealization of a typical stress-strain curve of a uniaxial tensile test on an elastoplastic material.

The segment A − B represents the elastic domain of the material behavior. The initial Young's modulus is given by the slope of this segment and remains constant in the elastic domain. Under elastic behavior, it is considered that there are no permanent deformations, and all strains can be recovered upon unloading. This elastic behavior ends when the yield stress σ_0 is met (point B). From this moment on, the material begins suffering permanent plastic strains. The material can also suffer hardening, i.e. the yield stress increases as the plastic strains accumulate. This can be seen in Fig. 1 in segment B − F. At point C, for example, the accumulated plastic strain is given by ε^p and the increase of the yield stress from σ_0 to σ_0^1. This increase continues until the material reaches the ultimate strength (point F) and fails.

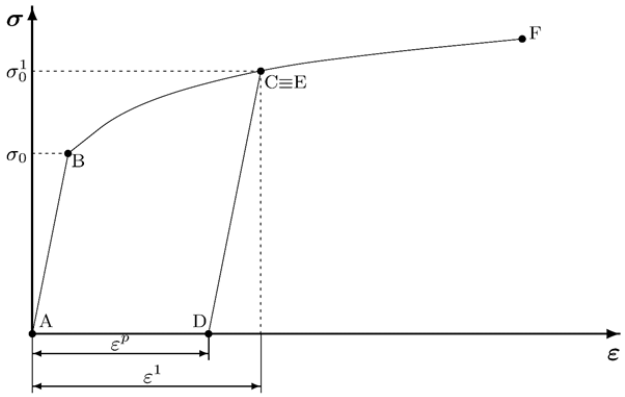

Fig. 1 Mathematical model of uniaxial tensile test

If the material is unloaded from point C, it will recover some of the accumulated strain, ε^1. In other words, at any given point of the loading curve under the plastic domain, the strain tensor can be decomposed in two components: one elastic (and thus recoverable) component, and one plastic (or permanent) component. For the uniaxial example in Fig. 1, the recovered elastic strain after unloading (segment C − D) is given by:

$$\varepsilon^e = \varepsilon^1 - \varepsilon^p \tag{1}$$

In the most general case, the strain tensor is decomposed according to

$$\varepsilon = \varepsilon^e + \varepsilon^p \tag{2}$$

where ε^e is the elastic strain tensor and ε^p is the plastic strain tensor.

In a uniaxial test, the yield stress is nothing but a scalar (Fig. 1). However, in a general three-dimensional case, the elastic domain is bounded by a yield surface instead. This surface is defined in the most general case by:

$$\Phi(\sigma, q) = 0 \tag{3}$$

where q represents a set of variables affected by the hardening (or softening) process. This scalar function delimits the region in the stress space where any point inside the surface, $\Phi < 0$, is in the elastic domain and any point on the surface, $\Phi = 0$, corresponds to plastic yielding.

As the hardening variables increase in value (or decrease), so will the yield surface expand (or shrink). This effect is known as isotropic hardening (or softening). In the most general case, the surface can even change its shape or translate in the stress space (kinematic hardening or softening).

A. Computational Implementation

In this section, in order to evaluate the effect of the variability of the RVE on the mechanical properties of composites, stiffness analyses are performed. As done for other algorithms [40], [41], the present algorithm is used to generate the RVEs of the transverse section of a composite lamina. The effective elastoplastic material from the properties of their constituents is then evaluated by finite element models.

Various finite element analysis with different fiber volume fraction RVEs is generated. For the elastic material behavior section, several papers are validated with different material behavior, RVE size, Fiber size, etc.

The overall integration algorithm as it was implemented in a UMAT subroutine of commercial finite element software ABAQUS [42] is presented in the flowchart of Fig. 2. It follows a typical implicit elastic predictor/return mapping procedure used by, for example, Souza-Neto [39]. It begins by computing an elastic trial stress state and up-to-date hardening variables. If the trial stress state is still inside the paraboloidal yield surface, then the increment is considered to be fully elastic; otherwise, the algorithm for the return mapping is executed. Upon convergence of the plastic multiplier, all state variables, stress tensor and plastic strain tensor are updated accordingly.

Finite element (FE) analysis was carried out using ABAQUS [42] under plane strain condition. In the ABAQUS model, both the matrix and the fibers were meshed using structured meshing technique with quad-dominated element shapes. The two-dimensional 4-node bilinear plane strain quadrilateral elements (CPE4) were chosen to mesh the fiber and the matrix. There were also a relatively small amount of 3-node linear plane strain triangle elements (CPE3) due to meshing technique used. Since each model has so many fibers, it is difficult and time-consuming to generate each RVE manually. Therefore, Python scripts have been written to generate and distribute fibers in the FE models of the RVEs in ABAQUS [42].

III. Analysis and Results

In this paper, the material that has been chosen to study is consisting of E-glass fibers and epoxy resin as a matrix. The properties have been reported and used by Fiedler et al. [43]. Both the matrix and the fiber are treated as isotropic for the 2D model. The elastic properties of the fiber and the matrix are shown in Table I, while Table II summarizes the plastic properties of epoxy measured from tensile tests by Fiedler et al. [43].

TABLE I
Material Constants for Constituents of the Composite

Constituent	Young's modulus	Poisson's ratio
Fiber	70 GPa	0.2
matrix	3.35 GPa	0.35

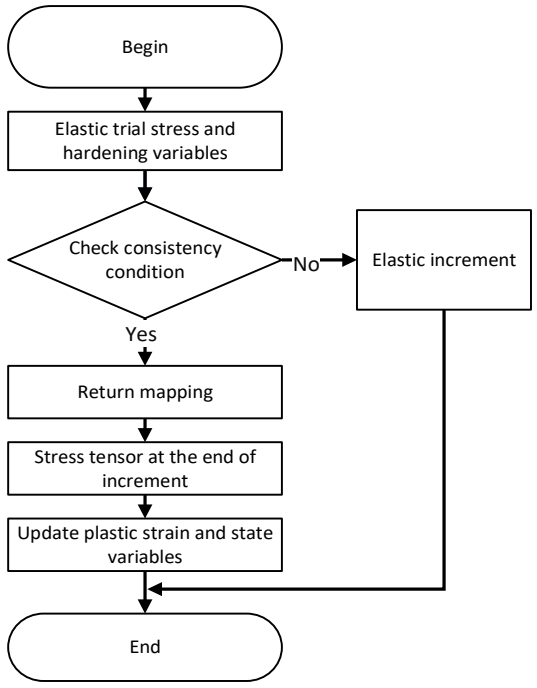

Fig. 2 Flowchart of implicit elastic predictor/return mapping algorithm

TABLE II
The Plastic Properties of Epoxy

$\varepsilon_p^e(\%)$	$\sigma_T(MPa)$	$\varepsilon_p^e(\%)$	$\sigma_T(MPa)$
0.00	29.0	0.85	81.5
0.03	37.0	1.02	84.5
0.06	45.0	1.20	87.0
0.13	52.0	1.41	89.0
0.19	58.0	1.62	91.0
030	65.0	1.81	92.5
0.39	70.0	2.04	93.5
0.53	74.0	2.27	94.5
0.69	78.0	2.50	95.0

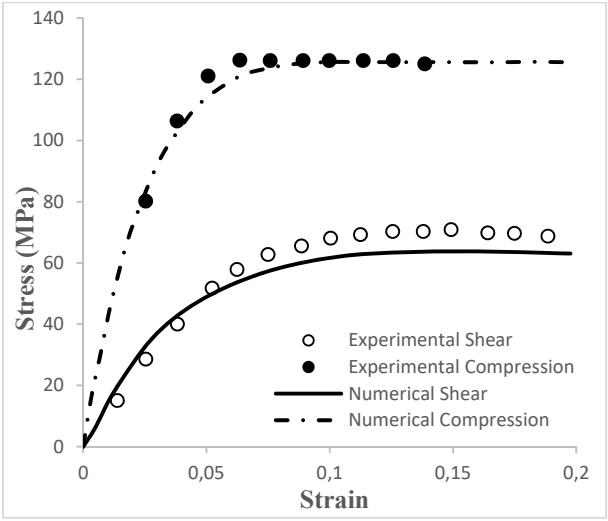

Fig. 3 Comparison of experimental data [43] with numerical results from matrix mesh

In order to verify the developed method with other solutions, several RVEs with different fiber distributions were generated. The elastoplastic constitutive model was implemented in a user subroutine UMAT in ABAQUS.

Two different unidirectional analyses were performed on a simple two-dimensional matrix mesh – tension and shear. In Fig. 3, the results are compared with the experimental data from Fiedler et al. [43]. Considering that tension result is in good agreement by default with the experimental data, since it is based on these values that the plastic behavior of the matrix is modeled. The numerical results for shear agree very well with the available experimental data, despite some under-prediction of the maximum stress.

For the next step, we tried to calculate the effective properties by using the homogenization method. The aim of this section is to calculate a relation between stress and plastic strain which can be used for introducing the new material in ABAQUS software for further analyses. Two methods for deriving these relations are used. In the first method, true stress and strain are obtained in terms of engineering stress and strain by (4) and (5).

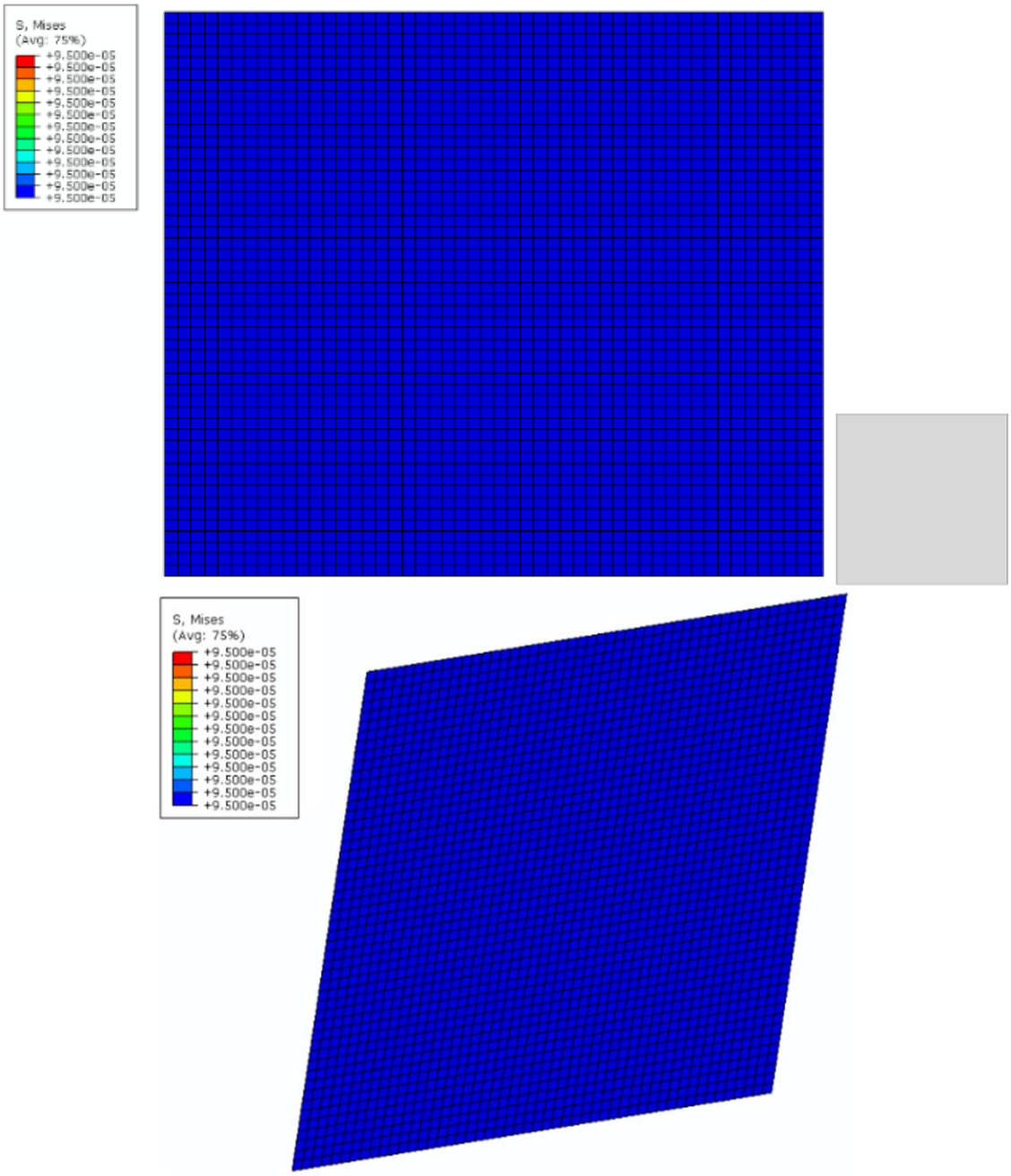

Fig. 4 RVE used to verify the developed method with the experimental data from Fiedler et al. [43]

It is important to note that (4) should only be used until the onset of necking. Beyond maximum load, the true stress

should be determined from actual measurements of load and cross-sectional area.

$$+\sigma_{tru}=\sigma_{nom}(1+\varepsilon_{nom}) \quad (4)$$

The true strain ε_{tru} may be determined from the engineering or conventional strain ε_{nom} by

$$\varepsilon_{tru}=\ln(1+\varepsilon_{nom}) \quad (5)$$

Then, the elastic module is obtained from

$$E=\sigma_{tru}(1)/\varepsilon_{tru}(1) \quad (6)$$

And at last, plastic strain is calculated by

$$\varepsilon_{pl} = \varepsilon_{tru} - \frac{\sigma_{tru}}{E} \quad (7)$$

Or the second method, the overall plastic strain can be derived directly by the homogenization of plastic strain in each integration points all over the model. The average plastic strain in an RVE is defined by:

$$\bar{\varepsilon}_{pl} = \frac{1}{V}\int_V \varepsilon_{pl} dV \quad (8)$$

These two methods are performed, and the results are compared with the input plastic behavior introduced in Table II. The results are illustrated in Fig. 5. It is found that the new model formulation is capable of providing an accurate prediction of the effective elastoplastic response of fiber reinforced composites.

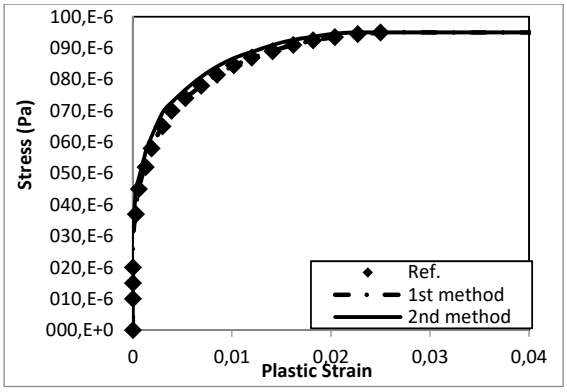

Fig. 5 Stress-plastic strain relationship for matrix

The next sections present a few examples of RVEs under different loading conditions and provide a better insight into the matrix material behavior defined by the present elastoplastic constitutive model.

Two loading conditions are presented: transverse tension and transverse shear. The elastic properties and plastic evolution data from Fiedler et al. [43] were used to model the epoxy mechanical behavior.

Since the goal of the current section is to provide an overview of the deduced elastoplastic constitutive model, different volume elements are chosen. Thus, the volume element has more than 10× the fiber radius in the transverse direction. The minimum interval between any two neighboring fibers is set to 0.1× the fiber radius, and the fiber volume fraction is set to 45%.

Several different fiber distributions were generated, and the different loading conditions mentioned above were applied on each distribution independently. Each case will be analyzed in detail in the following.

A. RVE with 45% Fiber Volume Fraction

Fig. 6 shows a RVE with 45% fiber volume fraction and the results obtained by applying transverse tension and shear load to it. Figs. 6 (B) and 8 (E) show the spatial distribution of the equivalent von-Mises for the generated fiber spatial distribution in transverse tension and shear loadings, respectively. Moreover, Figs. 6 (C) and 8 (F) illustrate the equivalent plastic strain for transverse tension and shear loadings, respectively. It can be seen that the regions of the matrix where the equivalent plastic strain is greater are located between those neighboring fibers aligned with the load direction (horizontal, in this case).

After homogenization is done, the effective material properties are calculated and used for analyzing the RVE with the homogenized material characteristic.

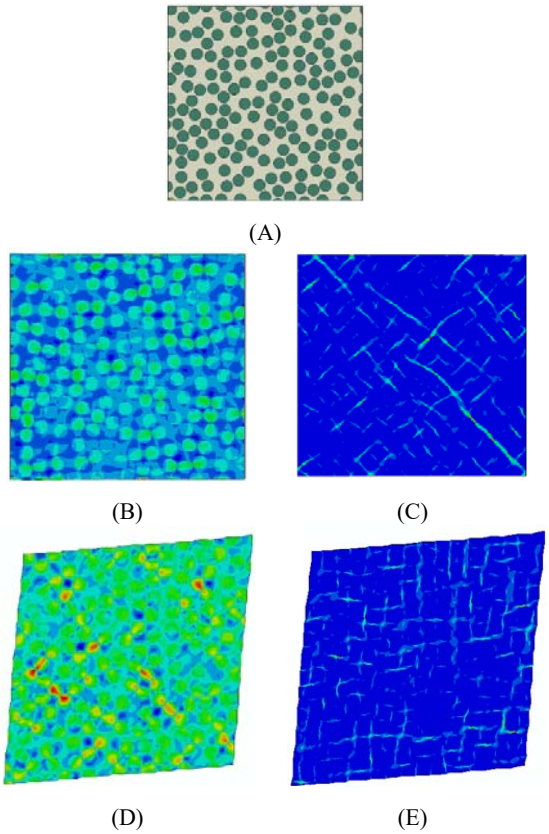

Fig. 6 RVEs with 45% fiber volume fraction (174 Fibers) under normal and shear loading (A) Modeling RVE, (B) Von-Mises stress contour under normal loading, (C) Equivalent plastic strain contour under normal loading, (D) Von-Mises stress contour under Shear loading, (E) Equivalent plastic strain contour under shear loading

In Fig. 7, the RVE with homogenized material properties, Von-Mises stress and equivalent plastic strain contours are presented for both transverse tension and shear loadings.

For RVEs with random fiber distribution and adequate fiber radii, the Von-Mises stress and equivalent plastic are not maximum just in a part of RVEs but also became to the maximum limit in so many spots. This is a good sign of acceptable fiber distribution.

Fig. 8 shows the transverse stress-strain curves obtained after volumetric homogenization for the fiber distribution. It can be seen that for the volume homogenization element, there is almost no scatter between RVE's and Homogenization curves.

In the next step, the true stress and strain relations described in the previous section are used to introduce the overall equivalent plastic strain and true stress relation. By this equivalent plastic strain and true stress relation, we can model the homogenized material instead of modeling an RVE with 45% fiber volume fraction which is used for the homogenized RVE in this section. Fig. 9 shows the relationship between equivalent plastic strain and true stress for an RVE with 45% fiber volume fraction. The relation between stress and plastic strain is obtained in a good agreement with the input data shown in Table II.

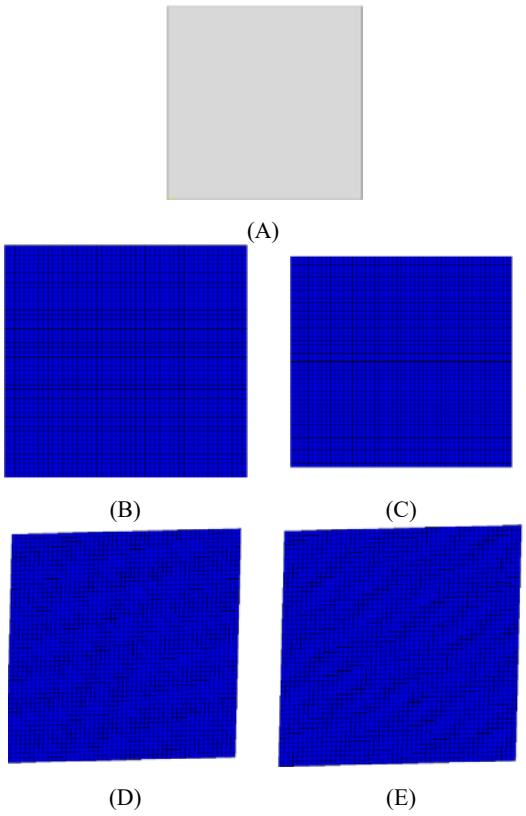

Fig. 7 RVEs with homogenized material properties under normal and shear loading (A) Modeling RVE, (B) Von-Mises stress contour under normal loading, (C) Equivalent plastic strain contour under normal loading, (D) Von-Mises stress contour under Shear loading, (E) Equivalent plastic strain contour under shear loading

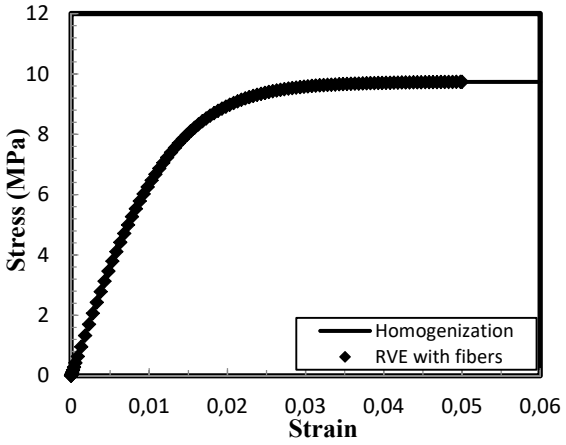

Fig. 8 The transverse stress-strain curves obtained after volumetric homogenization

B. RVE with 45% Fiber Volume Fraction and a Central Hole

In this section, we explore the size of RVE for different fiber arrangements and radius sizes. First, we analyzed the response of RVE of fibrous composites with an elastoplastic matrix and elastic fibers, subject to transverse normal and shear loadings. The numerical results obtained by analyzing the 2D RVEs generated with non-uniformly dispersed fibers and fully periodic boundary conditions, for various fiber arrangements and radius sizes, are presented subsequently.

In order to highlight the deformation of the generated RVEs and use of periodic boundary conditions for both normal and shear loading conditions, corresponding Von-Mises stress and equivalent plastic strain contours for all RVEs with non-uniform fiber dispersion are shown in Figs. 10-13. The applied strain for all normal and pure shear loading cases was 0.5%. The deformation of the RVEs reveals the accuracy of the applied PBCs and meshing scheme for both normal and shear loadings. The Von Mises stress contours reveal the expected variability of stress concentrations at the fiber/ matrix interfaces within the RVE resulting from the non-uniform fiber dispersion, while similarly, stress contours corresponding to shear loading simulations reveal the degree of non-uniformity. As it is shown in the figure, the Von-Mises stress and equivalent plastic strain contour maximize in many parts of RVE simultaneously, and that is because of both the high number of fibers in the RVE and the acceptable randomness of distributions. Furthermore, since there is a stress concentration in the each RVEs, the maximum values start in the vicinity of the central hole.

Computed volume averaged in-plane elastoplastic behaviors are compared for all the RVEs in both normal and shear loadings in Figs. 12 and 13. Fig. 12 shows a homogenized model in which only the fibers are omitted during the homogenization process, and the central hole still exists. Another homogenization step is done to eliminate the central hole (Fig. 13). In each homogenized model, different material properties are calculated in spite of the central hole.

Fig. 14 presents the equivalent plastic strain that defines effective material properties by homogenizing fibers and

central hole.

Figs. 15 and 16 present a comparison among computed the graphs of stress-strain values with five randomly generated non-uniform fiber dispersion morphologies and two RVE with two homogenized material properties, for 45% fiber volume fraction under transverse tension and shear loading. A negligible (e.g., 1%) standard deviation for different morphologies existed, demonstrating an excellent conversion in numerical results. The response of random microstructures converges well for large volume element size and predicts a more gradual transition from elastic response to plastic collapse than the simulations conducted on periodic RVEs.

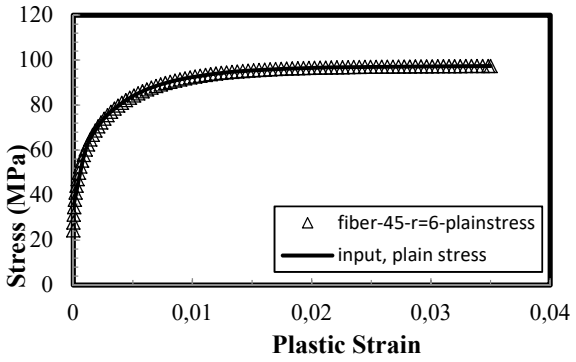

Fig. 9 Equivalent plastic strain and true stress relation for an RVE with 45% fiber volume fraction

We find that the plastic response of the composite is more sensitive to the geometry of the microstructure analyzed than the elastic response. So, a larger RVE is needed to investigate the elastoplastic response of fiber reinforced composite than elastic behavior.

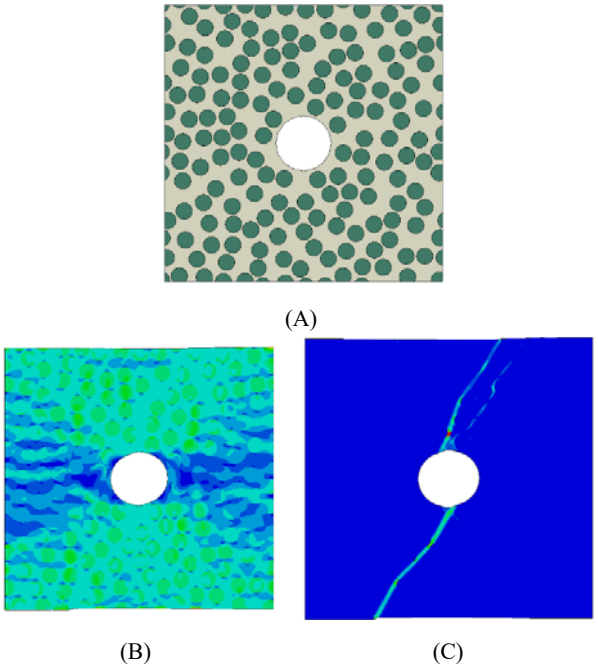

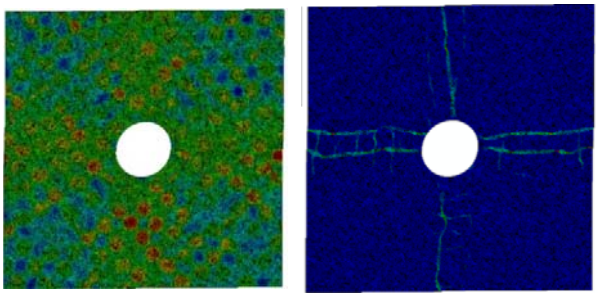

Fig. 10 RVEs with central hole and 45% fiber volume fraction (176 Fibers) under normal and shear loading (A) Modeling RVE, (B) Von-Mises stress contour under normal loading, (C) Equivalent plastic strain contour under normal loading, (D) Von-Mises stress contour under Shear loading, (E) Equivalent plastic strain contour under shear loading

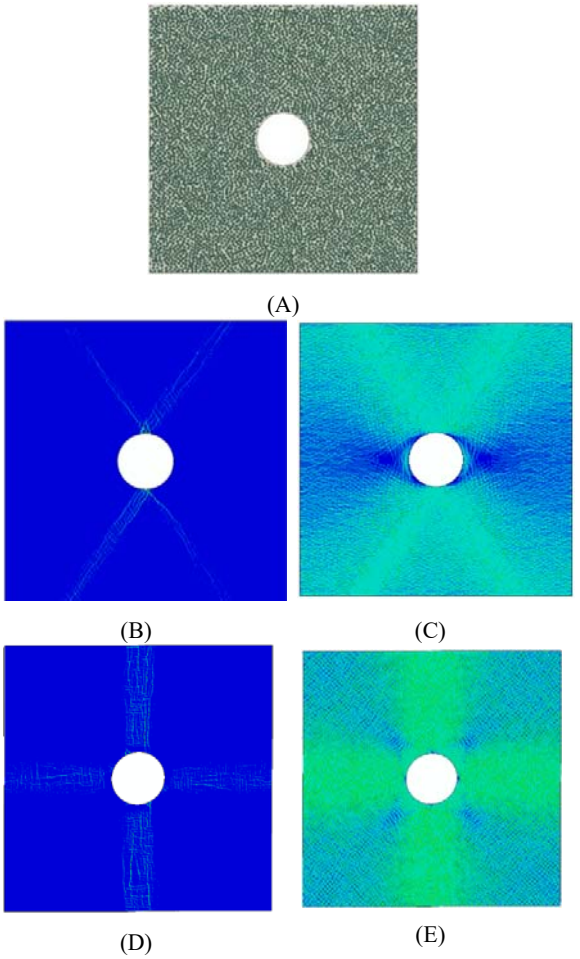

Fig. 11 RVEs with central hole and 45% fiber volume fraction (5718 Fibers) under normal and shear loading, (A) Modeling RVE, (B) Von-Mises stress contour under normal loading, (C) Equivalent plastic strain contour under normal loading, (D) Von-Mises stress contour under Shear loading, (E) Equivalent plastic strain contour under shear loading

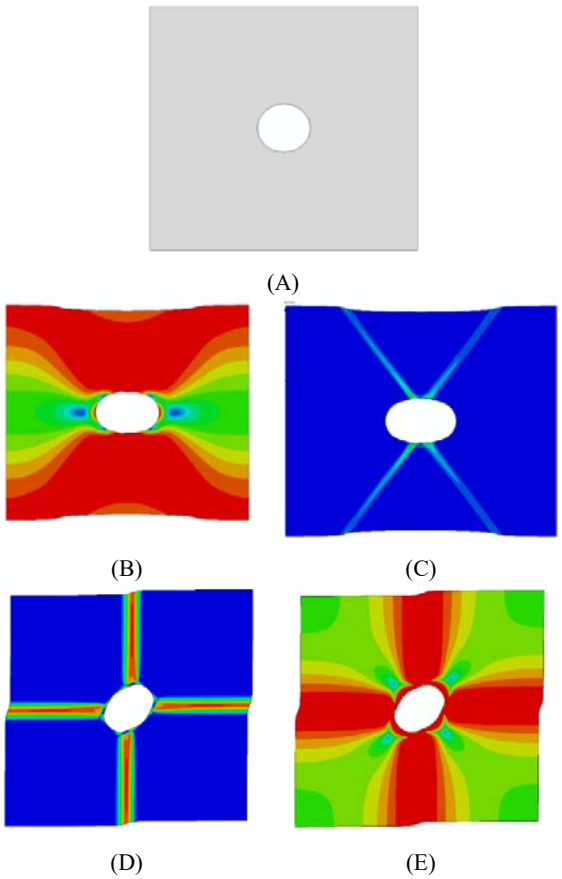

Fig. 12 RVEs with central hole and homogenized material properties under normal and shear loading, (A) Modeling RVE, (B) Von-Mises stress contour under normal loading, (C) Equivalent plastic strain contour under normal loading, (D) Von-Mises stress contour under Shear loading, (E) Equivalent plastic strain contour under shear loading

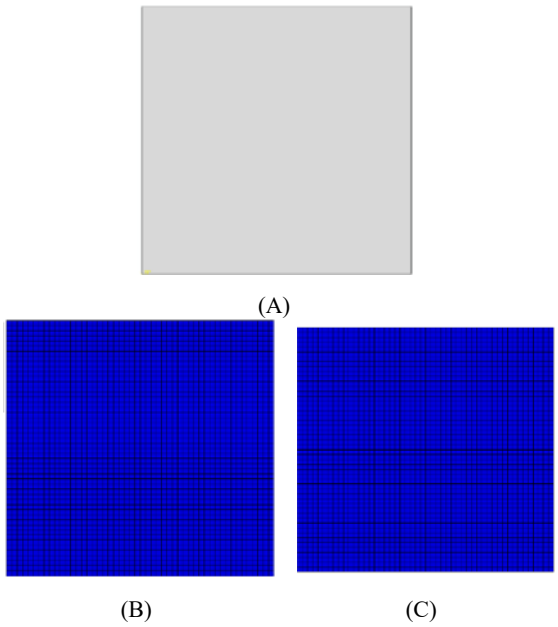

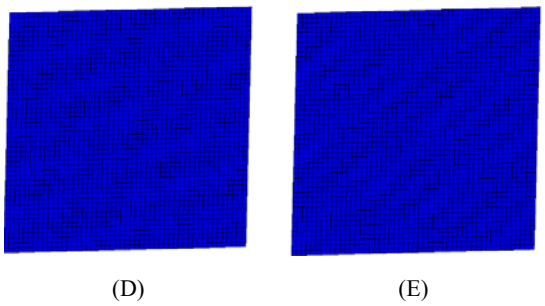

Fig. 13 RVEs with homogenized material properties under normal and shear loading, (A) Modeling RVE, (B) Von-Mises stress contour under normal loading, (C) Equivalent plastic strain contour under normal loading, (D) Von-Mises stress contour under Shear loading, (E) Equivalent plastic strain contour under shear loading

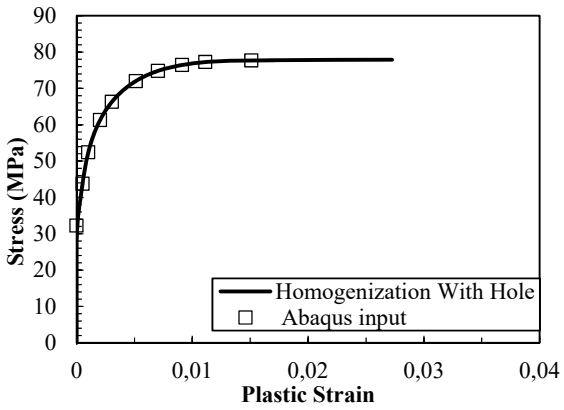

Fig. 14 Validation of the homogenization material properties with input data

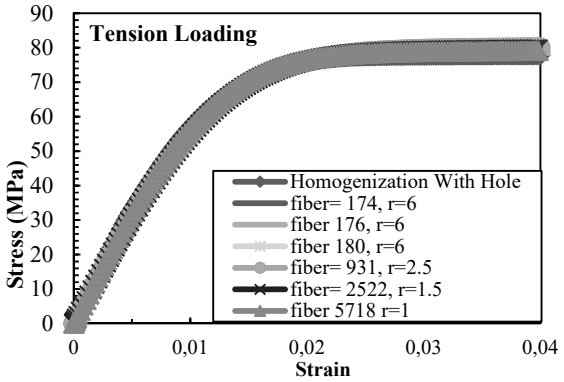

Fig. 15 Stress-strain relationship under tension loading

IV. Time Consumption (Computational Homogenization of Elastoplastic Composites)

Using such numerical calculations on RVE requires very large memory and time spending. Fig. 17 shows the evolution of the required time as a function of the number of fibers involved in the calculations for a personal computer with core i7 CPU and 8 GB RAM. The worst analysis corresponding to the higher values in time is clearly pointed out (number of fibers=5718). Fig. 17 described the time consumption of micromechanical analyses due to the number of fibers in the

RVEs.

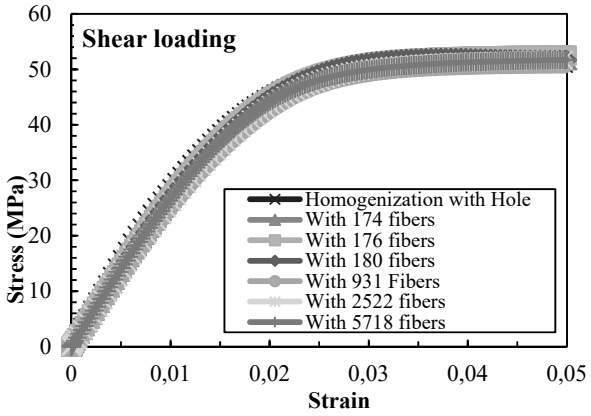

Fig. 16 Stress-strain relationship under shear loading

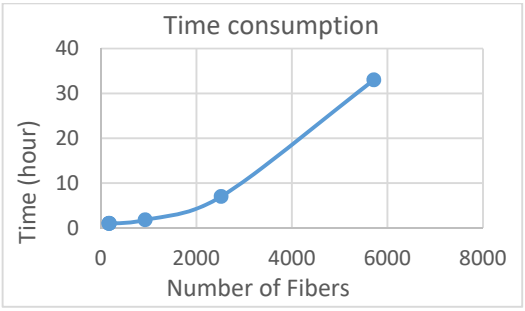

Fig. 17 Time required in hours as a function of the number of fibers

V. Conclusion

The present work investigates the effective properties and the microscopic deformation of the fibrous composite material. The effective material properties are calculated by the homogenization method, and the microscopic deformation is modeled by the FEM for RVEs with arbitrarily fiber distribution and fiber volume fractions. The conclusions can be summarized as follows:

. For validation, an RVE with resin properties is considered. Different analyses are done under normal and shear loadings and after homogenization, the effective material properties are derived and compared with other literature. The results were in a good agreement.

'. In the next step, some investigations on effective material properties of an RVE with 45% fiber volume fraction with arbitrarily fiber distribution is done. The results obtained by analyzing the model with homogenized material properties are in a good agreement compared to the original micromechanical RVE.

3. A new RVE with a central hole which represents stress concentration is considered next. The effect of stress concentration is investigated with RVEs with different fiber arrangements and radius sizes. Two types of homogenization are done. The first homogenization level is utilized to introduce new material properties instead of fiber and matrix. In the following, the second homogenization level is developed to eliminate the central hole. In this case, new effective material properties are calculated that replies fiber reinforced composite and also a central hole. In another word, it means a new RVE with only one material can model instead of the RVE with many fibers and a hole.

4. The same procedure is proposed for RVE with several holes to investigate the effect of several stress concentrations. Similar to the previous section, two levels of homogenization are successfully implemented to introduce an RVE with new effective material properties to omit the fibers and holes.

References

[1] Mishnaevsky Jr, Leon L. "Three-dimensional numerical testing of microstructures of particle reinforced composites." Acta Materialia 52.14 (2004): 4177-4188.

[2] González, C., J. Segurado, and J. LLorca. "Numerical simulation of elasto-plastic deformation of composites: evolution of stress microfields and implications for homogenization models." Journal of the Mechanics and Physics of Solids 52.7 (2004): 1573-1593.

[3] Pierard, O., et al. "Micromechanics of elasto-plastic materials reinforced with ellipsoidal inclusions." International Journal of Solids and Structures 44.21 (2007): 6945-6962.

[4] Tandon, G. P., and G. J. Weng. "A theory of particle-reinforced plasticity." Journal of Applied Mechanics 55.1 (1988): 126-135.

[5] Doghri, Issam, and Amine Ouaar. "Homogenization of two-phase elasto-plastic composite materials and structures: study of tangent operators, cyclic plasticity and numerical algorithms." International Journal of Solids and structures 40.7 (2003): 1681-1712.

[6] Bao, G., J. W. Hutchinson, and R. M. McMeeking. "Particle reinforcement of ductile matrices against plastic flow and creep." Acta metallurgica et materialia 39.8 (1991): 1871-1882.

[7] Delannay, Laurent, Issam Doghri, and O. Pierard. "Prediction of tension–compression cycles in multiphase steel using a modified incremental mean-field model." International Journal of Solids and Structures 44.22-23 (2007): 7291-7306.

[8] Chu, T. Y., and Zvi Hashin. "Plastic behavior of composites and porous media under isotropic stress." International Journal of Engineering Science 9.10 (1971): 971-994.

[9] Qiu, Y. P., and G. J. Weng. "A theory of plasticity for porous materials and particle-reinforced composites." Journal of Applied Mechanics 59.2 (1992): 261-268.

[10] Ju, J. W., and L. Z. Sun. "Effective elastoplastic behavior of metal matrix composites containing randomly located aligned spheroidal inhomogeneities. Part I: micromechanics-based formulation." International Journal of Solids and Structures 38.2 (2001): 183-201.

[11] Farrissey, L., et al. "Investigation of the strengthening of particulate reinforced composites using different analytical and finite element models." Computational materials science 15.1 (1999): 1-10.

[12] LLorca, J., and J. Segurado. "Three-dimensional multiparticle cell simulations of deformation and damage in sphere-reinforced composites." Materials Science and Engineering: A 365.1-2 (2004): 267-274.

[13] Sun, L. Z., and J. W. Ju. "Elastoplastic modeling of metal matrix composites containing randomly located and oriented spheroidal particles." Journal of applied mechanics 71.6 (2004): 774-785.

[14] Monetto, Ilaria, and W. J. Drugan. "A micromechanics-based nonlocal constitutive equation and minimum RVE size estimates for random elastic composites containing aligned spheroidal heterogeneities." Journal of the Mechanics and Physics of Solids 57.9 (2009): 1578-1595.

[15] Pensée, Vincent, and Q-C. He. "Generalized self-consistent estimation of the apparent isotropic elastic moduli and minimum representative volume element size of heterogeneous media." International journal of solids and structures 44.7-8 (2007): 2225-2243.

[16] Drugan, W. J., and J. R. Willis. "A micromechanics-based nonlocal constitutive equation and estimates of representative volume element size for elastic composites." Journal of the Mechanics and Physics of Solids 44.4 (1996): 497-524.

[17] Bulsara, V. N., Ramesh Talreja, and J. Qu. "Damage initiation under transverse loading of unidirectional composites with arbitrarily distributed fibers." Composites science and technology 59.5 (1999):

673-682.
[18] Rakow, Joseph F., and Anthony M. Waas. "The effective isotropic moduli of random fibrous composites, platelet composites, and foamed solids." Mechanics of Advanced Materials and Structures 11.2 (2004): 151-173.
[19] Swaminathan, Shriram, Somnath Ghosh, and N. J. Pagano. "Statistically equivalent representative volume elements for unidirectional composite microstructures: Part I-Without damage." Journal of Composite Materials 40.7 (2006): 583-604.
[20] Swaminathan, Shriram, N. J. Pagano, and Somnath Ghosh. "Analysis of interfacial debonding in three-dimensional composite microstructures." Journal of engineering materials and technology 128.1 (2006): 96-106.
[21] Kanit, T., et al. "Determination of the size of the representative volume element for random composites: statistical and numerical approach." International Journal of solids and structures 40.13-14 (2003): 3647-3679.
[22] Ranganathan, Shivakumar I., and Martin Ostoja-Starzewski. "Scaling function, anisotropy and the size of RVE in elastic random polycrystals." Journal of the Mechanics and Physics of Solids 56.9 (2008): 2773-2791.
[23] Elvin, A. A., and S. Shyam Sunder. "Microcracking due to grain boundary sliding in polycrystalline ice under uniaxial compression." Acta materialia 44.1 (1996): 43-56.
[24] Gusev, Andrei A. "Representative volume element size for elastic composites: a numerical study." Journal of the Mechanics and Physics of Solids 45.9 (1997): 1449-1459.
[25] Ostoja-Starzewski, Martin. "Material spatial randomness: From statistical to representative volume element." Probabilistic engineering mechanics 21.2 (2006): 112-132.
[26] Ren, Z-Y., and Q-S. Zheng. "A quantitative study of minimum sizes of representative volume elements of cubic polycrystals—numerical experiments." Journal of the Mechanics and Physics of Solids 50.4 (2002): 881-893.
[27] Zohdi, T. I., and P. Wriggers. "On the sensitivity of homogenized material responses at infinitesimal and finite strains." Communications in Numerical Methods in Engineering 16.9 (2000): 657-670.
[28] Salmi, Moncef, et al. "Various estimates of Representative Volume Element sizes based on a statistical analysis of the apparent behavior of random linear composites." Comptes Rendus Mécanique 340.4-5 (2012): 230-246.
[29] Soize, Christian. "Tensor-valued random fields for meso-scale stochastic model of anisotropic elastic microstructure and probabilistic analysis of representative volume element size." Probabilistic Engineering Mechanics 23.2-3 (2008): 307-323.
[30] Sab, Karam, and Boumediene Nedjar. "Periodization of random media and representative volume element size for linear composites." Comptes Rendus Mécanique 333.2 (2005): 187-195.
[31] Galli, Matteo, Joël Cugnoni, and John Botsis. "Numerical and statistical estimates of the representative volume element of elastoplastic random composites." European Journal of Mechanics-A/Solids 33 (2012): 31-38.
[32] Heinrich, C., et al. "The influence of the representative volume element (RVE) size on the homogenized response of cured fiber composites." Modelling and simulation in materials science and engineering 20.7 (2012): 075007.
[33] Salahouelhadj, A., and H. Haddadi. "Estimation of the size of the RVE for isotropic copper polycrystals by using elastic–plastic finite element homogenisation." Computational Materials Science 48.3 (2010): 447-455.
[34] Khisaeva, Z. F., and M. Ostoja-Starzewski. "On the size of RVE in finite elasticity of random composites." Journal of elasticity 85.2 (2006): 153.
[35] Pelissou, C., et al. "Determination of the size of the representative volume element for random quasi-brittle composites." International Journal of Solids and Structures 46.14-15 (2009): 2842-2855.
[36] Hill, Rodney. The mathematical theory of plasticity. Vol. 11. Oxford university press, 1998.
[37] Kachanov, Lazar′ Markovich. Fundamentals of the Theory of Plasticity. Courier Corporation, 2004.
[38] Lubliner, Jacob. Plasticity theory. Courier Corporation, 2008.
[39] De Souza Neto, Eduardo A., Djordje Peric, and David RJ Owen. Computational methods for plasticity: theory and applications. John Wiley & Sons, 2011.
[40] Yang, Lei, et al. "A new method for generating random fibre distributions for fibre reinforced composites." Composites Science and Technology 76 (2013): 14-20.
[41] Vaughan, T. J., and C. T. McCarthy. "A combined experimental-numerical approach for generating statistically equivalent fibre distributions for high strength laminated composite materials." Composites Science and Technology 70.2 (2010): 291-297.
[42] Abaqus, Inc. "ABAQUS theory and standard user's manual." (2003).
[43] Fiedler, B., et al. "Failure behavior of an epoxy matrix under different kinds of static loading." Composites Science and Technology 61.11 (2001): 1615-1624.